Heliyon 8 (2022) e10961

Contents lists available at ScienceDirect

Heliyon

journal homepage: www.cell.com/heliyon

Research article

Understanding of mobility limiting factors in solution grown Al doped ZnO thin film and its low temperature remedy

Biswajit Mahapatra, Sanjit Sarkar *

Department of Physics, Surendranath Evening College, Kolkata 700009, India

ARTICLE INFO

Keywords:
Resistivity
Mobility
Surface adsorbed
Orange emission
AZO

ABSTRACT

The solution grown doped ZnO based transparent electrode has shown great potential in future generation flexible and smart devices due to its abundance in earth, low cost, simple and low temperature synthesis process. But solution grown doped ZnO possesses one major drawback, its mobility decreases rapidly with an increase in doping concentration. To eliminate this issue, the understanding of factors that limiting mobility is a prerequisite. But till date, there are very limited resources with detailed understanding of mobility limiting factors in solution grown TCO. Here in this report, with the morphological, optical and electrical investigations, the mobility limiting factor comes out to be surface related property and assigned to be the defects related to surface adsorbed oxygen and oxygen species at the surface. Furthermore, we have modified the surface to remove the surface adsorbed oxygen species by a low temperature (70 °C) simple solution process. Surface modified sample shows more than two orders of improvement in resistivity without any significant change in the transparency in visible range.

1. Introduction

The demand for efficient transparent conducting oxides (TCOs) is increasing exponentially which is further fuelled by its wide range of optoelectronic applications, such as transparent electronic devices e.g. LEDs [1, 2], front contact of electronic flat panel display [3], thin film transistor [4, 5], chemical sensors [6] and most importantly transparent front contact in Si solar cells [7, 8, 9]. To be a good candidate for practical use in the industrial devices, the TCO should posses the properties like high electrical conductivity, higher optical transparency in the visible spectral range and stability against hostile environment [10, 11]. Tin doped In_2O_3 (ITO) is the leading commercially used TCO materials till date due to its satisfactory electrical and optical properties for the optoelectronic device applications. Till date, the search for the low cost and earth abundant alternative of the conventional ITO was still continuously developed due to the toxicity and scarcity of Indium in earth [12]. On the other hand, aluminium doped zinc oxide (AZO) has drawn much attention of research community due to their large band-gap energy of >3 eV and comparable resistivity of the order of 10^{-4} Ω-cm. Apart from low production cost, ZnO possesses many other advantages such as: non-toxicity, excellent thermal and chemical stability against hostile environment [13, 14].

There are plenty of reports on the different doping process of AZO such as Radio frequency magnetron sputtering [15], pulsed laser deposition [16], atomic layer deposition [17], etc. But most of the techniques involve either costly instruments, higher orders of vacuum or the synthesis procedures are very complicated. On the other hand, to decrease the resistivity, most of the synthesis processes require high temperature growth or high temperature post growth annealing treatment which makes the procedure unsuitable for TCO deposition on flexible substrates [18, 19]. Several groups have reported lower resistivity after post growth treatment. Lee et al. [20] have observed a 3 times decrease in resistivity after post growth annealing at 600 °C. Gao et al. [21] have reported up to three order decrease in resistivity due to reduction process in presence of hydrogen atmosphere at 400 °C. Basically all the post growth treatments are done at higher temperature (400 °C to 700 °C). So, it is not possible to apply post growth annealing treatment for TCO on flexible substrates. Recently, Mickan et al. [15] have reported highly conductive AZO by reactive high impulse magnetron sputtering method at room temperature. In recent days, researchers are interested in flexible devices even wearable electronic devices for which the low temperature grown TCO is mandatory. In this regard, researchers are in search for a low cost easy synthesis method to synthesize TCO at a temperature <100 °C.

Solution grown method is a simple low cost thin film deposition technique by which uniform large area AZO thin film can be produced at large scale. Apart from the various advantages, it has one major

* Corresponding author.
E-mail address: snjtsarkar0@gmail.com (S. Sarkar).

https://doi.org/10.1016/j.heliyon.2022.e10961
Received 22 June 2022; Received in revised form 3 September 2022; Accepted 30 September 2022

drawback. The mobility of solution grown AZO thin film decreases rapidly with an increase in Al doping which limits the conductivity [22]. However, the clear understanding of the mobility limiting factors in solution grown AZO is missing in the literature. On the other hand, to improve the mobility and conductivity, understanding of mobility limiting factors is a prerequisite.

Therefore, in this report, we have investigated solution grown AZO thin film and demonstrated the in-depth understanding of mobility limiting factors. We further demonstrated a surface engineering method, by which the resistivity of the as grown AZO can be reduced by more than two orders at a temperature 80 °C without any significant change in transparency in the visible (400–800 nm) range. To the best of our knowledge, this is the first report about more than two orders improvement in resistivity by post growth treatment at a temperature bellow 100 °C.

2. Experimental methods

ZnO and AZO thin films were deposited by sol-gel spin coating technique on the glass substrate as reported earlier [22]. Briefly, the sol was prepared by taking 0.1 M of zinc acetate di-hydrate in dehydrated isopropyl alcohol with the addition of 0.1 M diethanolamine. The solution was then vigorously stirred for 1 h and kept it for 2 days to check the stability of the sol. For different concentration of Al doping, required amount aluminum nitrate was added to the sol during continuous stirring. Thin films are deposited on ultra-sonically cleaned glass substrate by spin coating technique. All the samples are further modified by sulfur treatment by dipping in a 10 mM solution of thioacetamide for 1 h at the temperature 80 °C. Then the samples are dried in an oven at a temperature 80 °C for 2 h. To evaluate the exact reason behind the mobility enhancement we have performed 1, 3, 5, and 7 h sulfur treatment of the 1% Al doped sample.

The investigation regarding crystalline phase was carried by X-ray diffractometer (XRD, Seifert, model: XDAL 3000), surface and morphological characterization was carried out be Field Emission Scanning Electron Microscopy (FESEM; JEOL 2100F) and elemental mapping was carried out by high resolution transmission electron microscopy (HRTEM, model JEM2010). X-ray photoelectron spectroscopy was done by XPS instrument (Omicron: Serial no. 0571). The room temperature emission spectra were recorded using a He–Cd laser (Kimmon Koha Co., Ltd.; model KR1801C) with 325 nm laser excitation source, a Newport monochromator with an attached photomultiplier tube (Horiba Jobin Yvon, Model: iHR 320). The absorbance spectra are measured by UV–VIS spectrophotometer (Parkin Elmer, Model: Lamda 35; Serial no. 101N6022703). Room temperature Hall measurement was performed in Ecopia Hall Measurement System (Model: HMS 3000).

3. Result and discussions

The X-ray diffraction (XRD) patterns of undoped and doped samples are shown in Figure 1. All the samples show diffraction peaks corresponds to wurtzite phase of ZnO [23, 24]. No other phase of ZnO or Al_2O_3

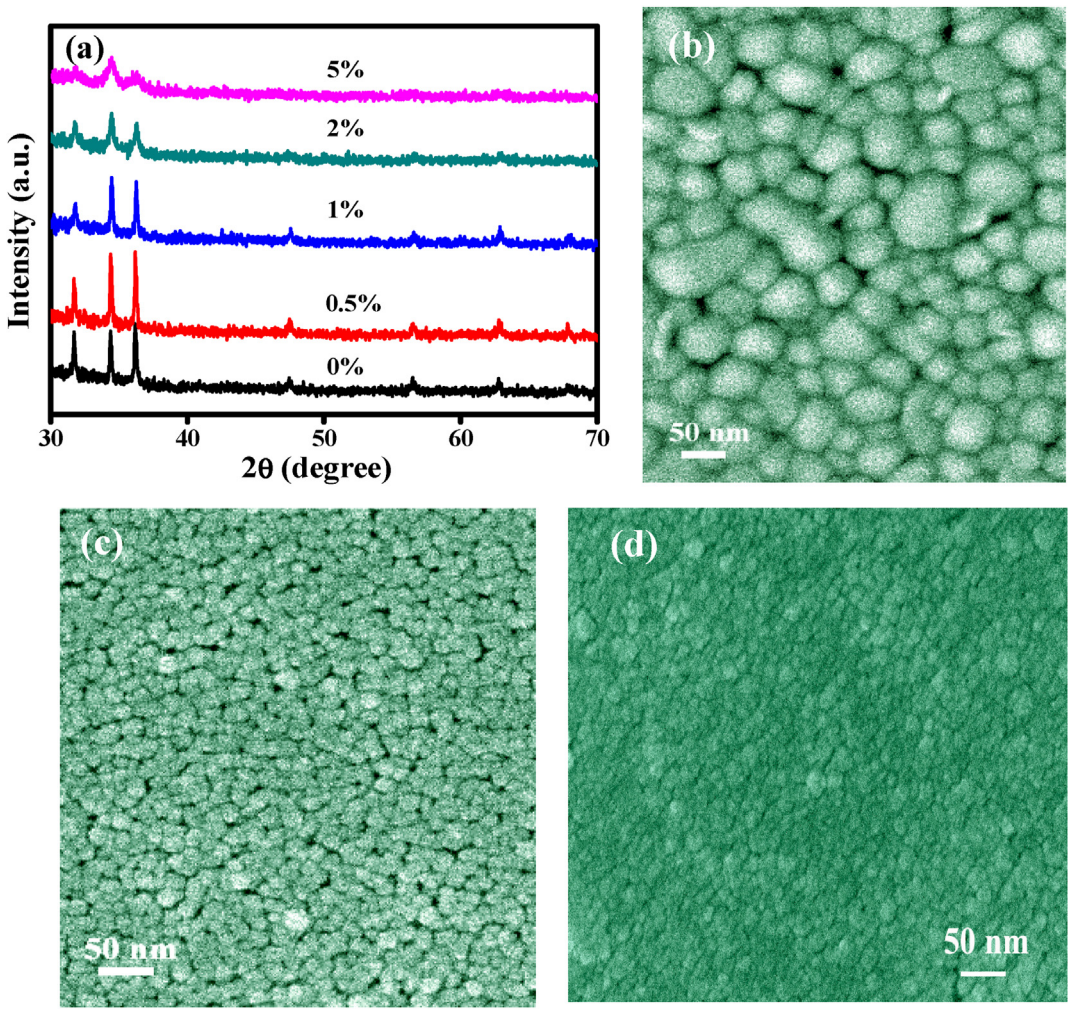

Figure 1. (a) X-ray diffraction pattern of undoped and Al doped ZnO thin film, (b), (c) and (d) are the FESEM images of undoped, 1% Al doped and 5% Al doped ZnO respectively.

has been observed which ensures the doping of Al in the ZnO crystals. The intensity of the peaks decreases with an increase in Al doping concentration. That might be due to the degradation of crystalline quality as Al doping concentration increases. Similar degradation in crystal quality due to Al doping has been observed by Mahroug et al. [25] and Li et al. [26] Interestingly the 002 peak shows a right shift for the samples with 1% of Al doped or more (shown in supplementary information, Figure S1). This shift indicates the doping of Al in the crystallite site. As the effective ionic radius of Al^{3+} (53.5 pm) is less than that of Zn^{2+} (74 pm), therefore according to linear Vegard's law, we may expect a higher angle shift of 002 peak when Zn is substituted by Al [27, 28].

The FESEM images of the representative samples are shown in Figure 1(b)–(d). As the Al content increases, the grain size decreases. The grain size of undoped sample is irregular and varies from 17 nm to 115 nm and which becomes uniform with size ~20 to 25 nm in case of 1% Al doped sample. The grain size becomes <20 nm in case of 5% Al doped ZnO sample. The change in grain size with an increase in Al content also observed by Mridha et al. [22] and Shrinatha et al. [29].

The transmittance spectra of the samples are shown in Figure 2(a). All the samples show more than 85% transmittance throughout the visible range of wavelength (400–800 nm) irrespective their doping concentration whereas commercial ITO shows transparency of 80–85% in 400–800 nm wavelength regions [30]. The absorption edge is shifted towards shorter wavelength with an increase in Al doping concentration. We have calculated the optical band gap (Shown in table TS1 of supplementary information) and found to be increasing with an increase in Al doping concentration. This shifting is due to the Burstein–Moss effect [31]. The room temperature photoluminescence spectra of the samples

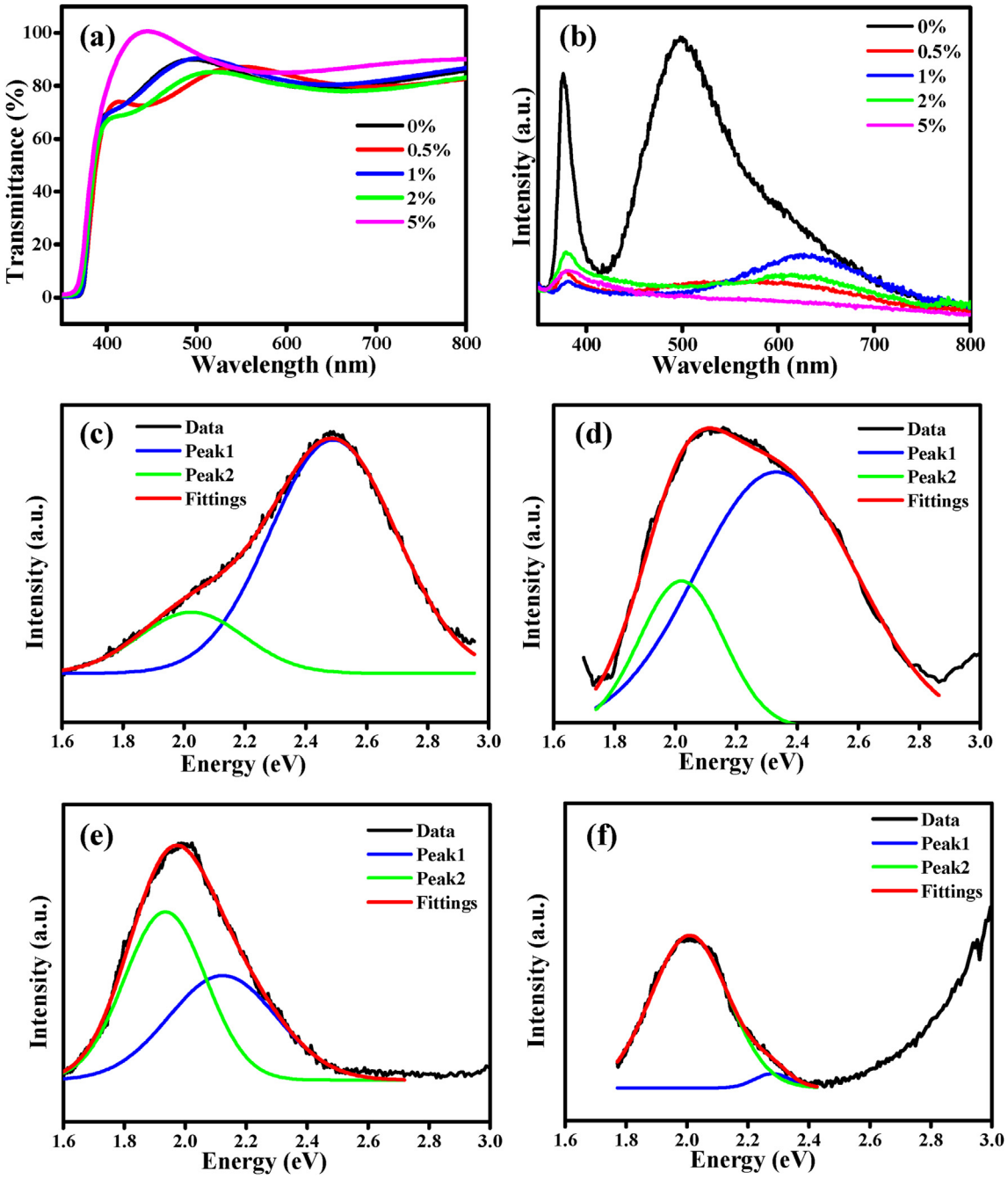

Figure 2. (a) UV–Vis transmittance spectra of all the samples. (b) RTPL spectra of the samples. (c)–(f) are the Gaussian multi peak fittings of the visible emissions of undoped and 0.5%, 1% and 2% Al doped samples respectively.

Table 1. Ratio of visible and orange emission with doping concentration.

Sample (% Al doping)	$I_{visible}/I_{orange}$
0	3.2
0.5	2.03
1	0.61
2	0.63

are shown in Figure 2(b). Undoped ZnO thin film shows a sharp and strong UV emission centered at 380 nm and a broad comparable visible emission centered 500 nm. The UV emission intensity decreases with an increase in Al doping concentration. The visible emission also decreases as Al doping concentration increases. Similar decrease in emission quality due to Al doping also reported by Wang et al. [32] and Sahal et al. [33] Interestingly visible emission peak position shifts towards longer wavelength and orange emission dominates in case of 1% and 2% Al doped samples. For better understanding, we have deconvoluted the visible emission peak (Figure 2(c)–(f)) and found that relative contribution of orange emission peak to the total visible emission increases up to 2% Al doped sample (Table 1). The relative contribution of orange emission peak (~2 eV) increases rapidly with an increase in Al doping concentration up to 1%. Then there is no significant change between 1% and 2% Al doped sample. For 5% Al doped sample emission is so poor therefore de-convolution could not be performed. It is well established that the visible emission in ZnO is due to the presence of defects [34, 35]. Therefore, as the visible emission peak shifts from green to orange, we may expect the change in defect types.

The electrical properties of the samples are shown in Figure 3. The carrier concentration increases from 4.38×10^{16} for undoped ZnO to 1.03×10^{19} for 1% Al doped sample. Beyond 1% Al doping, the carrier concentration decreases a little. Similar phenomenon also has been observed by Mridha et al. [22] and Banerjee et al. [36] for Al doped ZnO.

The resistivity and mobility of the samples are shown in Figure 3(b) and (c). Resistivity value decreases from 86.79 Ω-cm for ZnO and attains a minimum value of 3.69 Ω-cm for 1% Al doped ZnO and it increases slowly for higher doping concentration. The resistivity values are higher than the commercial TCO ($\sim 10^{-4}$). This is because low temperature and air ambient synthesis procedure creates lots of surface defects and scattering centres at the grain boundaries. Other hand, low activation of dopants at low temperature processing might be the reason [37]. The change in carrier concentration is more than three orders but the decrease in resistivity is only one order in case of 1% Al doped sample. This difference of two orders in resistivity and carrier concentration is due to the rapid decrease in mobility with an increase in Al doping concentration. The mobility decreases with an increase in Al doping concentration and attains a minimum value of 0.16 $cm^2 V^{-1} s^{-1}$ for 1% Al doping from 1.66 $cm^2 V^{-1} s^{-1}$ in case of undoped ZnO sample i.e. more than one order decrease in case of 1% Al doped sample than that of undoped sample.

The mobility in doped metal oxide is described by Matthiessen's rule:

$$\frac{1}{\mu} = \sum_i \frac{1}{\mu_i} = \frac{1}{\mu_{impurity}} + \frac{1}{\mu_{gb}} + \frac{1}{\mu_{hopping}} + \frac{1}{\mu_{phonon}} + \ \ldots\ldots\ldots$$

where $\mu_{impurity}$, μ_{gb}, $\mu_{hopping}$, and μ_{phonon} are the mobility limiting factors that influence mobility from impurity scattering, scattering at grain boundary, retardation by hopping transport, and phonon scattering, respectively. Ionized impurity scattering increases with the increase in doping concentration and hence limited the mobility in doped metal oxide thin films. Cornelius et al. [38] have described that the mobility of Al doped ZnO compact thin films are either controlled by ionized impurity scattering or grain boundary limited transport depending upon the free electron density. Steinhauser et al. [39] have reported that the mobility is limited by grain boundary contribution in low carrier regime and controlled by intra-grain mobility limiting factors for carrier concentration $\sim 10^{20}$. Elmar et al. [40] also reported that for carrier concentration $\sim 10^{19}$, the mobility is governed by grain boundary effects. Considering the carrier concentration ~ 10^{18} and the change in grain size with Al

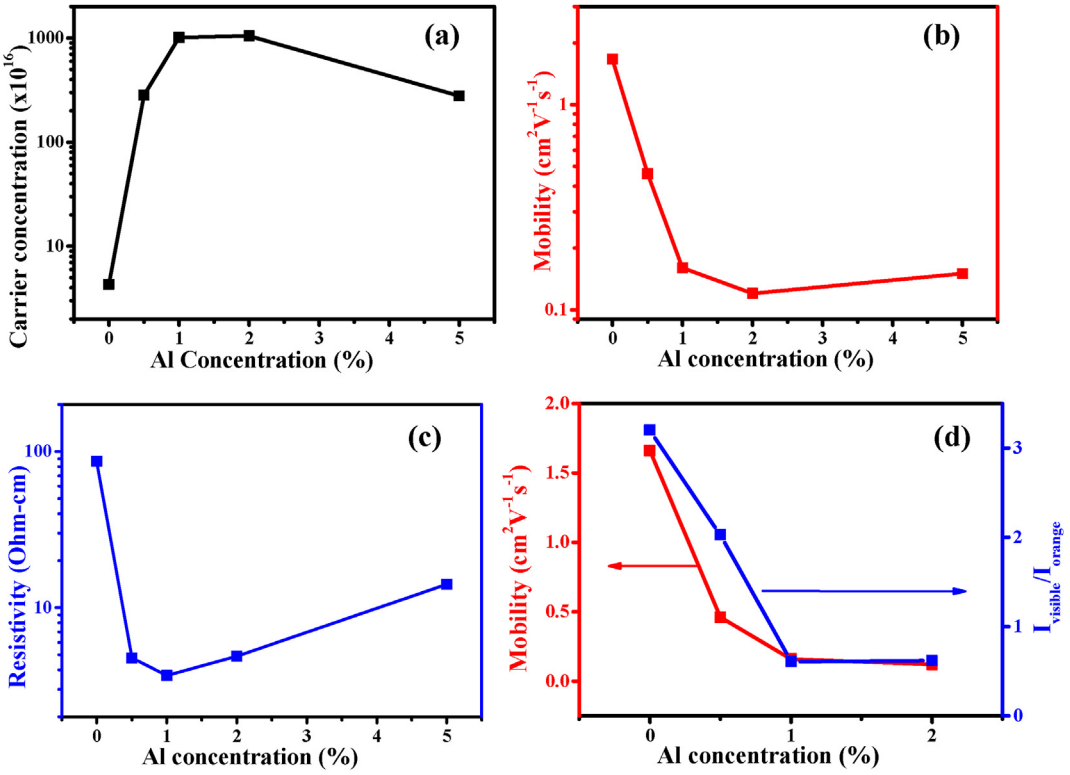

Figure 3. Hall measurement of the samples (Van der Paw method). (a) Carrier concentration, (b) Carrier mobility, (c) Resisticity of undoped and doped samples. (d) Change in carrier mobility and relative change of orange emission with the change in doping concentration.

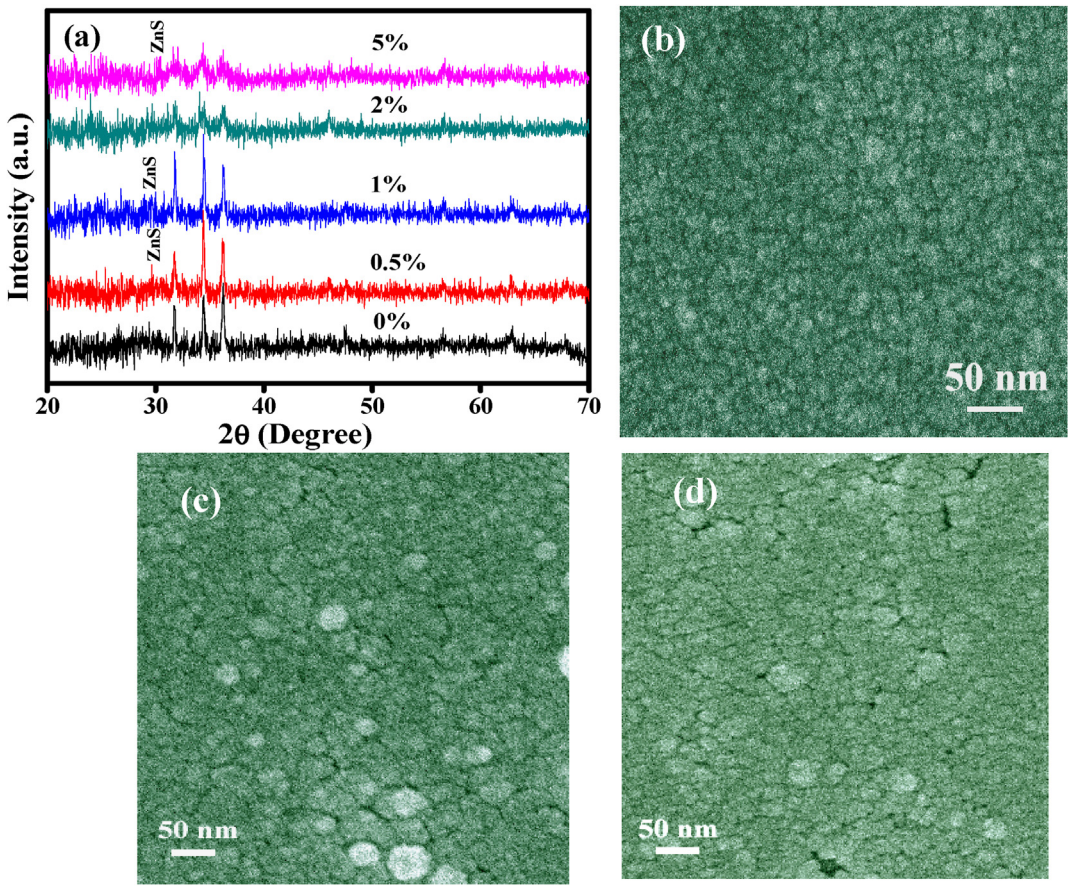

Figure 4. (a) XRD patterns of the sulfur treated samples. (b), (c) and (d) are the FESEM images of the samples undoped, 1%, and 5% Al doped samples after sulfur treatment.

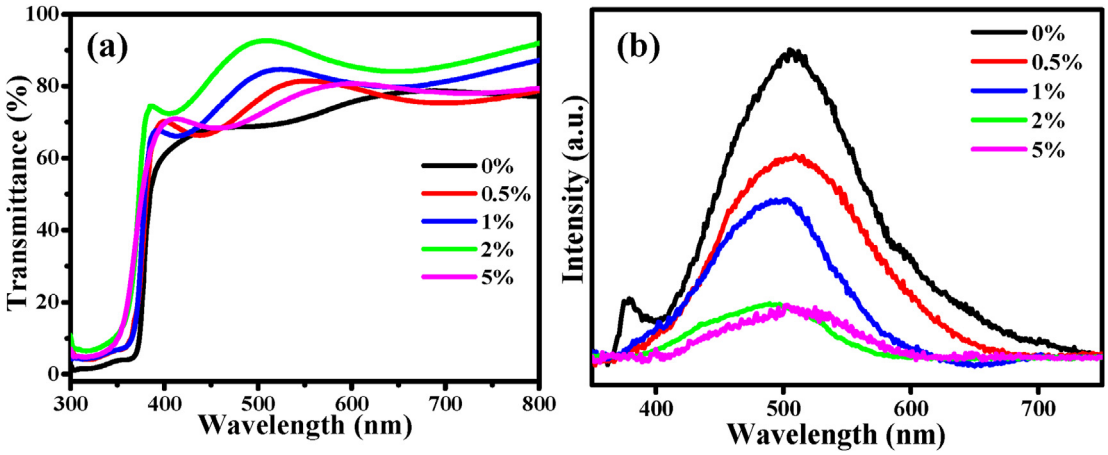

Figure 5. (a) Absorption and (b) Photoluminescence spectra of the samples after sulfur treatment.

doping concentration, we can conclude that the mobility in our solution grown samples is grain boundary limited. According to Seto model the mobility in grain boundary limited conduction is governed by Eq. (1):

$$\mu = \mu_0 \exp(-\Phi_B / KT) \quad (1)$$

where μ_0 is in-grain mobility and Φ_B is the potential barrier at grain boundary. Therefore, the change in barrier height at the grain boundary can be the reason behind lower carrier mobility in higher doping regime. Interestingly, the gradual decrease in carrier mobility and the gradual increase in orange emission as the doping concentration increases indicate some close relationship between orange emission and carrier mobility. The relative contribution of orange emission increases in a similar manner of decrease in carrier concentration (Figure 3(d)). The Orange emission in solution grown ZnO is very common and origin of which is still controversial. There are reports who assigned interstitial oxygen (O_i) as the source of orange emission [41, 42]. In contrary Djurisic et al. [43] have reported surface adsorbed species like O_2^-, OH^- are responsible for the orange emission in solution grown ZnO and Fan et al. [44] reported that the chemisorbed oxygen or other oxygen-containing species (e.g., OH^-) are responsible for yellow orange emission.

Now, as the Al doping concentration increases, the formation of O_i is favorable due to the charge neutralization tendency of the crystal [26]. On the other hand the crystallite size decreases as the Al doping concentration increases i.e. the surface to volume ratio increases. Therefore, we may expect an increase in surface adsorbed oxygen species. Therefore, decrease in carrier mobility might be either due to increase in O_i in the crystal or due to increase in surface to volume ratio i.e. chemisorbed oxygen species.

Fan et al. [44] also reported the orange emission is due to chemisorbed oxygen or hydroxyl groups which are further responsible for band bending at the surface of ZnO nanostructures. In air ambient, the surface of solution grown ZnO nanostructure is covered by ionized oxygen species and hydroxyl groups. These surface defects trap free electrons from the conduction band and create depletion region at the surface of ZnO [44]. This negative charge distribution at the surface causes upward shifting of the conduction band. The barrier height Φ_B depends on the amount of surface traps and hence limited the mobility according to the Seto formula [45].

To evaluate the exact reason, we have modified the surface of ZnO to remove chemisorbed oxygen species from the surface. If our proposition of chemisorbed oxygen species is right then any surface modification to remove the surface traps will reduce the barrier height and as a consequence the mobility will be enhanced. Therefore, we have performed post growth surface modification by developing a thin ZnS layer on the doped and undoped ZnO. The structural and morphological characterizations (Figure 4(a)–(d)) indicate the formation of ZnS layer over ZnO and without any such significant change in morphology. In case of modified samples, the XRD peak intensity corresponding to ZnO wurtzite phase decreases sharply. This indicates that due to the ionic exchange the crystalline quality of the ZnO film surface degrades. In modified samples, the 002 peak of ZnO is slightly shifted to the higher 2θ angle. The shift might be due to the change in stress in the crystal and the change in defect states at the surface. Higher angle shift of 002 peak of ZnO due to the crystal stress also have been reported by Fang et al. [46] Along with the peaks of ZnO, a small hump around 2θ value 29.3° has been observed in case of sulfur treated samples. This peak is identified as 111 peak of cubic ZnS as reported by Panigrahi et al. [47] However the intensity is very poor. This indicates that there might be a very thin coating of ZnS over ZnO thin film or the coating is mostly amorphous in nature. To be confirmed about the formation of ZnS over ZnO, we have performed the elemental mapping by transmission electron microscopy. The mapping shows presence of Zn, Al, O and S which confirms the formation of ZnS over ZnO (Figure S2 of Supplementary Information). The presence of comparable S atoms along with Zn, O and Al further confirms the proposition that crystalline quality of ZnS is poor. The poor crystalline quality of ZnS over ZnO synthesized by solution growth has also been reported by Lin et al. [48].

The absorbance spectra of the samples are shown in Figure 5(a). It is clear that the formation of ZnS layer on ZnO have not degraded the transmittance of the samples significantly. All the samples show more than 80% transparency in the visible region which is almost comparable to the transparency of commercial TCO (80–85% in 400–800 nm of illumination). Interestingly the room temperature PL spectra (Figure 5(b)) show the absence of orange red emission for all the samples which is in good agreement with our proposition. Again the emission quality degrades as the Al doping concentration increases. The increase in green emission is due to the formation of $ZnO_{1-x}S_x$ at the interface. This emission is in well agreement with our previous report [49] and Panigrahi et al. [47].

The electrical measurements of modified samples are shown in Figure 6(a)–(c). The carrier concentration of the treated samples shows increases from 4.38×10^{16} for untreated to 8.34×10^{17} in sulfur treated ZnO sample. But in case of 1% Al doped sample, Carrier concentration decreases a little whereas for higher doping concentration the carrier concentration decreases more. The resistivity of the samples maintains the same trend like untreated samples but with decreased values of more than one order as shown in Table 2.

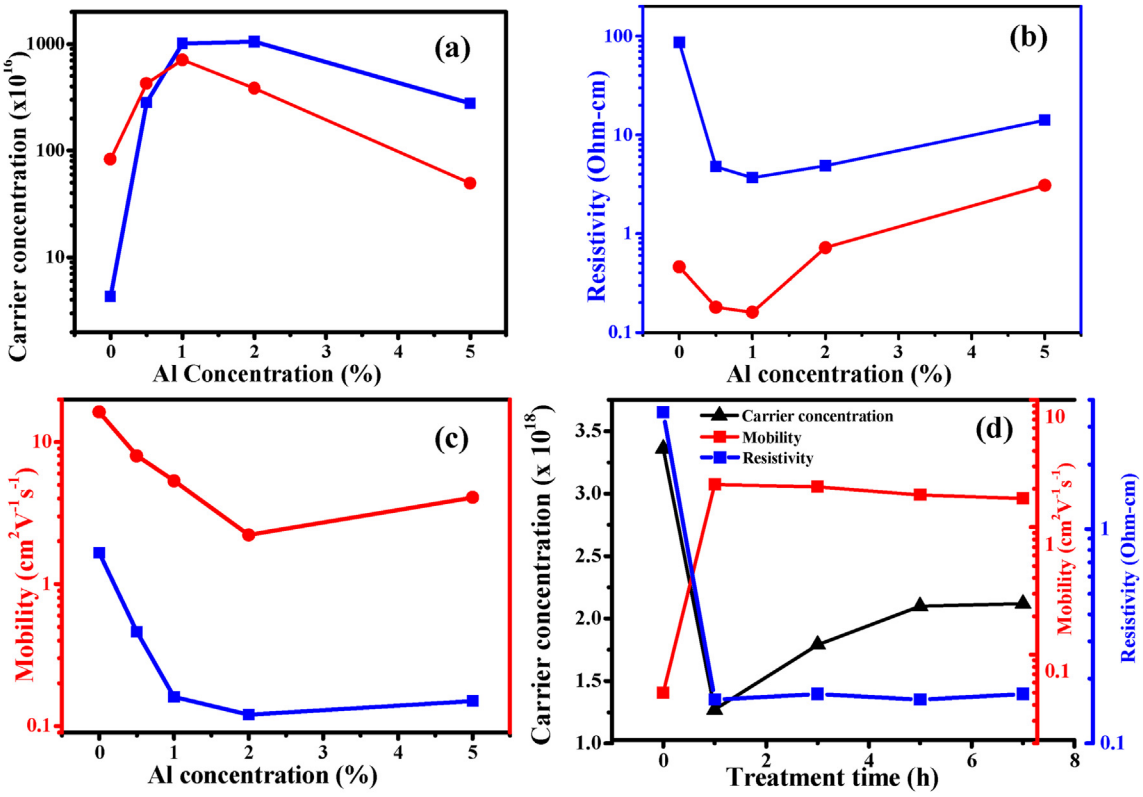

Figure 6. Electrical measurement of the samples before and after sulfur treatment. (a) Carrier concentration, (b) resistivity and (c) carrier mobility. (d) Variation of electrical parameters with sulfur treatment time.

Table 2. Electrical measurements of the samples, before and after sulfur treatment.

Al doping (%)	As grown			After sulphur treatment		
	n ($\times 10^{16}$)	μ (cm^2 V^{-1} s^{-1})	ρ (Ohm-cm)	n ($\times 10^{16}$)	μ (cm^2 V^{-1} s^{-1})	ρ (Ohm-cm)
0.0	4.31	1.66	86.79	83.4	16.27	0.46
0.5	283	0.46	4.77	426	7.99	0.18
1.0	1010	0.16	3.69	710	5.33	0.16
2.0	1050	0.12	4.9	385	2.21	0.72
5.0	277	0.15	14.3	49.5	4.08	3.08

For ZnO sample resistivity value decreases to 0.46 Ω-cm from 86.79 Ω-cm and that for 1% Al doepd sample decreases to 0.16 Ω-cm from 3.69 Ω-cm due to sulfur treatment. That is the resistivity decreases more than two orders due to sulfur treatment. The mobility of 1% Al doped sample increases from 0.16 cm^2 $V^{-1}s^{-1}$ to 5.33 cm^2 $V^{-1}s^{-1}$. This high mobility is comparable to the mobility reported for high temperature processed Al doped ZnO [50, 51, 52]. Nearly 33 times enhancement in mobility due to surface modification further confirms our proposition that mobility in solution grown ZnO is governed by grain boundary and particularly in this case, mobility is governed by the surface defects related to the chemisorbed oxygen species.

To be further confirmed about surface dependency of mobility, we have varied the surface modification time from zero to 7 h (Figure 6(d)) and found that all the changes in carrier concentration, resistivity and mobility are happening just within 1 h of modification process. For further modification time, mobility decreases a little. The changes in orange emission over sulfur treatment time (Shown in Figure S3 of Supplementary Information) clearly show that the changes in orange emission is wiped out within 1 h of treatment although there is no such significant change in other visible emission. This result further confirms that the mobility in solution grown ZnO is governed by the defects responsible for orange emission in ZnO i.e. surface absorbed oxygen related trap states.

4. Conclusions

Here, in this report, we have investigated the reason of low carrier mobility in solution grown Al doped ZnO nanocrystalline thin film. With the help of structural and photoluminescence characterization, we have established that the defect responsible for orange emission is responsible for low carrier mobility in nanocrystalline ZnO thin film. We also have proposed a novel low temperature (80 °C) remedy to modify AZO surface by sulfur treatment and observed more than two orders of improvement in resistivity and more than one order improvement in mobility and hence resistivity of the AZO films. The sulfur treated samples show enhanced mobility as well as reduced orange red emission. The enhancement in mobility is highest for highest carrier concentration which leaves us the scope to modify the existing ZnO based TCO surface to get higher mobility and lowest resistivity. This approach will be very much beneficial to improve the mobility and resistivity of AZO deposited on flexible substrate where high temperature treatment is not possible.

Declarations

Author contribution statement

Biswajit Mahapatra: Performed experiments; Analyzed and interpreted the data.

Sanjit Sarkar: Conceived and designed the experiments; Contributed reagents, materials analysis tools; Wrote the paper.

Funding statement

This work was supported by the Science & Engineering Research Board, New Delhi, India (EEQ/2018/000491).

Data availability statement

Data will be made available on request.

Declaration of interests statement

The authors declare no conflict of interest.

Additional information

Supplementary content related to this article has been published online at https://doi.org/10.1016/j.heliyon.2022.e10961.

Acknowledgements

Dr. S. Sarkar would like to thank Prof. Durga Basak for her guidance and experimental facilities.

References

[1] X. Jiang, F.L. Wong, M.K. Fung, S.T. Lee, Aluminum-doped zinc oxide films as transparent conductive electrode for organic light-emitting devices, Appl. Phys. Lett. 83 (2003) 1875–1877.
[2] N.F. Wang, Y.Z. Tsai, F.H. Hsu, Effect of surface texture on Al-Y codoped ZnO/n-Si heterojunction solar cells, IEEE Trans. Electron. Dev. 60 (2013) 4073–4078.
[3] K. Ellmer, Past achievements and future challenges in the development of optically transparent electrodes, Nat. Photonics 6 (2012) 808–816.
[4] E. Fortunato, P. Barquinha, R. Martins, Oxide semiconductor thin-film transistors: a review of recent advances, Adv. Mater. 24 (2012) 2945–2986.
[5] D.C. Paine, B. Yaglioglu, Z. Beiley, S. Lee, Amorphous IZO-based transparent thin film transistors, Thin Solid Films 516 (2008) 5894–5898.
[6] K. Sankarasubramanian, P. Soundarrajan, K. Sethuraman, K. Ramamurthi, Chemical spray pyrolysis deposition of transparent and conducting Fe doped CdO thin films for ethanol sensor, Mater. Sci. Semicond. Process. 40 (2015) 879–884.
[7] J. Muller, B. Rech, J. Springer, M. Vanecek, TCO and light trapping in silicon thin film solar cells, Sol. Energy 77 (2004) 917–930.
[8] A. Rayerfrancis, P.B. Bhargav, N. Ahmed, S. Bhattacharya, B. Chandra, S. Dhara, Sputtered AZO thin films for TCO and back reflector applications in improving the efficiency of thin film a-Si:H solar cells, Silicon 9 (2017) 31–38.
[9] T. Fujibayashi, T. Matsui, M. Kondo, Improvement in quantum efficiency of thin film Si solar cells due to the suppression of optical reflectance at transparent conducting oxide/Si interface by TiO2/ZnO antireflection coating, Appl. Phys. Lett. 88 (2006), 183508.
[10] L. Zhang, Y.J. Zhou, L. Guo, W.W. Zhao, A. Barnes, H.T. Zhang, C. Eaton, Y.X. Zheng, M. Brahlek, H.F. Haneef, N.J. Podraza, M.H.W. Chan, V. Gopalan, K.M. Rabe, R. Engel-Herbert, Correlated metals as transparent conductors, Nat. Mater. 15 (2016) 204–210.
[11] K.R. Poeppelmeier, J.M. Rondinelli, CORRELATED OXIDES Metals amassing transparency, Nat. Mater. 15 (2016) 132–134.
[12] H.K. Park, S.W. Yoon, W.W. Chung, B.K. Min, Y.R. Do, Fabrication and characterization of large-scale multifunctional transparent ITO nanorod films, J. Mater. Chem. 1 (2013) 5860–5867.
[13] A. Catellani, A. Ruini, A. Calzolari, Optoelectronic properties and color chemistry of native point defects in Al:ZnO transparent conductive oxide, J. Mater. Chem. C 3 (2015) 8419–8424.
[14] H.R. Choi, S.K. Eswaran, S.M. Lee, Y.S. Cho, Enhanced fracture resistance of flexible ZnO:Al thin films in situ sputtered on bent polymer substrates, ACS Appl. Mater. Interfaces 7 (2015) 17569–17572.
[15] M. Mickan, U. Helmersson, H. Rinnert, J. Ghanbaja, D. Muller, D. Horwat, Room temperature deposition of homogeneous, highly transparent and conductive Al-doped ZnO films by reactive high power impulse magnetron sputtering, Sol. Energy Mater. Sol. Cell. 157 (2016) 742–749.
[16] K.H. Kim, E.S. Lee, S.H. Lee, Highly transparent and low resistivity Al-doped ZnO thin films grown by pulsed laser deposition under different oxygen flow rates, in: Z.Y. Jiang, Y.H. Kim (Eds.), Nanotechnology and Precision Engineering, Pts 1 and 2 662, Trans Tech Publications Ltd, Stafa-Zurich, 2013, pp. 453–458.
[17] Y. Li, R. Yao, H.H. Wang, X.M. Wu, J.Z. Wu, X.H. Wu, W. Qin, Enhanced performance in Al-doped ZnO based transparent flexible transparent thin-film transistors due to oxygen vacancy in ZnO film with Zn-Al-O interfaces fabricated by atomic layer deposition, ACS Appl. Mater. Interfaces 9 (2017) 11711–11720.
[18] K.K. Kim, S. Niki, J.Y. Oh, J.O. Song, T.Y. Seong, S.J. Park, S. Fujita, S.W. Kim, High electron concentration and mobility in Al-doped n-ZnO epilayer achieved via dopant activation using rapid-thermal annealing, J. Appl. Phys. 97 (2005).
[19] J.P. Lin, J.M. Wu, The effect of annealing processes on electronic properties of sol-gel derived Al-doped ZnO films, Appl. Phys. Lett. 92 (2008), 134103.
[20] J.-H. Lee, K.-H. Ko, B.-O. Park, Electrical and optical properties of ZnO transparent conducting films by the sol–gel method, J. Cryst. Growth 247 (2003) 119–125.
[21] M. Gao, X. Wu, J. Liu, W. Liu, The effect of heating rate on the structural and electrical properties of sol–gel derived Al-doped ZnO films, Appl. Surf. Sci. 257 (2011) 6919–6922.

[22] S. Mridha, D. Basak, Aluminium doped ZnO films: electrical, optical and photoresponse studies, J. Phys. D Appl. Phys. 40 (2007) 6902–6907.
[23] R. Bhardwaj, A. Bharti, J.P. Singh, K.H. Chae, N. Goyal, S. Gautam, Structural and electronic investigation of ZnO nanostructures synthesized under different environments, Heliyon 4 (2018), e00594.
[24] H. Liu, Y. Ding, M. Somayazulu, J. Qian, J. Shu, D. Häusermann, H.-k. Mao, Rietveld refinement study of the pressure dependence of the internal structural parameter u in the wurtzite phase of ZnO, Phys. Rev. B 71 (2005), 212103.
[25] A. Mahroug, S. Boudjadar, S. Hamrit, L. Guerbous, Structural, optical and photocurrent properties of undoped and Al-doped ZnO thin films deposited by sol–gel spin coating technique, Mater. Lett. 134 (2014) 248–251.
[26] J. Li, J. Xu, Q. Xu, G. Fang, Preparation and characterization of Al doped ZnO thin films by sol–gel process, J. Alloys Compd. 542 (2012) 151–156.
[27] M.N. Magomedov, On the deviation from the Vegard's law for the solid solutions, Solid State Commun. 322 (2020), 114060.
[28] S.T. Khlayboonme, W. Thowladda, Impact of Al-doping on structural, electrical, and optical properties of sol-gel dip coated ZnO:Al thin films, Mater. Res. Express 8 (2021), 076402.
[29] N. Srinatha, P. Raghu, H.M. Mahesh, B. Angadi, Spin-coated Al-doped ZnO thin films for optical applications: structural, micro-structural, optical and luminescence studies, J. Alloys Compd. 722 (2017) 888–895.
[30] A. Axelevitch, Hot-probe characterization of transparent conductive thin films, Materials 14 (2021) 1186.
[31] A.D. Trolio, E.M. Bauer, G. Scavia, C. Veroli, Blueshift of optical band gap in c-axis oriented and conducting Al-doped ZnO thin films, J. Appl. Phys. 105 (2009), 113109.
[32] M. Wang, K.E. Lee, S.H. Hahn, E.J. Kim, S. Kim, J.S. Chung, E.W. Shin, C. Park, Optical and photoluminescent properties of sol-gel Al-doped ZnO thin films, Mater. Lett. 61 (2007) 1118–1121.
[33] M. Sahal, B. Hartiti, A. Ridah, M. Mollar, B. Mari, Structural, electrical and optical properties of ZnO thin films deposited by sol-gel method, Microelectron. J. 39 (2008) 1425–1428.
[34] C.H. Ahn, Y.Y. Kim, D.C. Kim, S.K. Mohanta, H.K. Cho, A comparative analysis of deep level emission in ZnO layers deposited by various methods, J. Appl. Phys. 105 (2009).
[35] M.K. Lee, H.F. Tu, Enhancement of ultraviolet and visible emissions of ZnO with Zn by thermal treatment, Jpn. J. Appl. Phys. 47 (2008) 980–982.
[36] P. Banerjee, W.-J. Lee, K.-R. Bae, S.B. Lee, G.W. Rubloff, Structural, electrical, and optical properties of atomic layer deposition Al-doped ZnO films, J. Appl. Phys. 108 (2010), 043504.
[37] K.-m. Lin, H.-C. Chen, Y.-Y. Chen, K.-y. Chou, Influences of preferred orientation growth on electrical properties of ZnO:Al films by sol–gel method, J. Sol. Gel Sci. Technol. 55 (2010) 369–376.
[38] S. Cornelius, M. Vinnichenko, N. Shevchenko, A. Rogozin, A. Kolitsch, W. Möller, Achieving high free electron mobility in ZnO:Al thin films grown by reactive pulsed magnetron sputtering, Appl. Phys. Lett. 94 (2009), 042103.
[39] J. Steinhauser, S. Faÿ, N. Oliveira, E. Vallat-Sauvain, C. Ballif, Transition between grain boundary and intragrain scattering transport mechanisms in boron-doped zinc oxide thin films, Appl. Phys. Lett. 90 (2007), 142107.
[40] K. Ellmer, R. Mientus, Carrier transport in polycrystalline ITO and ZnO:Al II: the influence of grain barriers and boundaries, Thin Solid Films 516 (2008) 5829–5835.
[41] C.H. Ahn, Y.Y. Kim, D.C. Kim, S.K. Mohanta, H.K. Cho, A comparative analysis of deep level emission in ZnO layers deposited by various methods, J. Appl. Phys. 105 (2009), 013502.
[42] B.G. Zhai, Y.M. Huang, Origin of thermal annealing-induced orange emissions from solution-grown ZnO nanocrystals, Mater. Res. Innov. 19 (2015) s45–s50.
[43] A.B. Djurisic, Y.H. Leung, Optical properties of ZnO nanostructures, Small 2 (2006) 944–961.
[44] J. Fan, F. Güell, C. Fábrega, A. Fairbrother, T. Andreu, A.M. López, J.R. Morante, A. Cabot, Visible photoluminescence components of solution-grown ZnO nanowires: influence of the surface depletion layer, J. Phys. Chem. C 116 (2012) 19496–19502.
[45] J.Y.W. Seto, The electrical properties of polycrystalline silicon films, J. Appl. Phys. 46 (1975) 5247–5254.
[46] Z.B. Fang, Z.J. Yan, Y.S. Tan, X.Q. Liu, Y.Y. Wang, Influence of post-annealing treatment on the structure properties of ZnO films, Appl. Surf. Sci. 241 (2005) 303–308.
[47] S. Panigrahi, S. Sarkar, D. Basak, Metal-free doping process to enhance the conductivity of zinc oxide nanorods retaining the transparency, ACS Appl. Mater. Interfaces 4 (2012) 2709–2716.
[48] H. Lin, L. Wei, C. Wu, Y. Chen, S. Yan, L. Mei, J. Jiao, High-performance self-powered photodetectors based on ZnO/ZnS core-shell nanorod arrays, Nanoscale Res. Lett. 11 (2016) 420.
[49] S. Sarkar, A. Das Mahapatra, D. Basak, Self-powered highly enhanced broad wavelength (UV to visible) photoresponse of ZnO@ZnO1−xSx@ZnS core–shell heterostructures, J. Colloid Interface Sci. 523 (2018) 245–253.
[50] F. Ruske, M. Roczen, K. Lee, M. Wimmer, S. Gall, J. Hüpkes, D. Hrunski, B. Rech, Improved electrical transport in Al-doped zinc oxide by thermal treatment, J. Appl. Phys. 107 (2010), 013708.
[51] Z. Zhan, J. Zhang, Q. Zheng, D. Pan, J. Huang, F. Huang, Z. Lin, Strategy for preparing Al-doped ZnO thin film with high mobility and high stability, Cryst. Growth Des. 11 (2011) 21–25.
[52] C. Agashe, O. Kluth, J. Hüpkes, U. Zastrow, B. Rech, M. Wuttig, Efforts to improve carrier mobility in radio frequency sputtered aluminum doped zinc oxide films, J. Appl. Phys. 95 (2004) 1911–1917.